



# Binary and Long#Term (Triple?) Modulations of 4U 1820–30 in NGC 6624

## Citation

Chou, Y., and J. E. Grindlay. 2001. "Binary and Long#Term (Triple?) Modulations of 4U 1820–30 in NGC 6624." *The Astrophysical Journal* 563 (2): 934–40. <https://doi.org/10.1086/324038>.

## Permanent link

<http://nrs.harvard.edu/urn-3:HUL.InstRepos:41399863>

## Terms of Use

This article was downloaded from Harvard University's DASH repository, and is made available under the terms and conditions applicable to Other Posted Material, as set forth at <http://nrs.harvard.edu/urn-3:HUL.InstRepos:dash.current.terms-of-use#LAA>

## Share Your Story

The Harvard community has made this article openly available.  
Please share how this access benefits you. [Submit a story](#).

[Accessibility](#)

## BINARY AND LONG-TERM (TRIPLE?) MODULATIONS OF 4U 1820–30 IN NGC 6624

Y. CHOU AND J. E. GRINDLAY

Harvard-Smithsonian Center for Astrophysics, 60 Garden Street, Cambridge, MA 02138; yichou@cfa.harvard.edu

Received 2001 June 16; accepted 2001 August 27

### ABSTRACT

We present timing analysis results for *Rossi X-Ray Timing Explorer* (*RXTE*) observations of X-ray binary source 4U 1820–30 located in the globular cluster NGC 6624. The light curves of observations made between 1996 October and 1997 September show that the maximum of the 685 s binary period modulation folded by the linear ephemeris from previous observations has a phase shift of  $-0.20 \pm 0.06$ . Combined with historical results (1976–1997), the binary period derivative is measured to be  $\dot{P}/P = (-3.47 \pm 1.48) \times 10^{-8} \text{ yr}^{-1}$ . The previous known ( $\sim 176$  day) long-term modulation is significant in the X-ray light curve obtained by analysis of the *RXTE* All-Sky Monitor (ASM) during the years 1996–2000. The *RXTE* ASM ephemeris is extended by analysis of all historical data (*Vela 5B* and *Ginga*) to yield a period of  $171.033 \pm 0.326$  days with no evidence for period change ( $|\dot{P}/P| < 2.20 \times 10^{-4} \text{ yr}^{-1}$ ). All reported X-ray burst activity is confined to within  $\pm 23$  days of the predicted minima. This stable long-term modulation is consistent with 4U 1820–30 being a hierarchical triple system with a  $\sim 1.1$  day period companion.

*Subject headings:* accretion, accretion disks — stars: individual (4U 1820–30) — X-rays: stars

### 1. INTRODUCTION

The low-mass X-ray binary 4U 1820–30 near the center of the globular cluster NGC 6624 (Grindlay et al. 1984) has a binary orbital period of 685.0118 s (Stella, Priedhorsky, & White 1987a; Smale, Mason, & Mukai 1987; Morgan, Remillard, & Garcia 1988; Sansom et al. 1989; Tan et al. 1991; van der Klis et al. 1993a, 1993b) and was the first X-ray burster identified with a known X-ray source (Grindlay et al. 1976). Its short orbital period and its X-ray burst activity imply that it is a system with a  $0.06\text{--}0.08 M_{\odot}$  helium white dwarf secondary star accreting mass onto a primary neutron star (Rappaport et al. 1987). A 176 day period long-term variation by factor of  $\sim 3$  between high luminosity and low luminosity was observed by the *Vela 5B* spacecraft (Priedhorsky & Terrell 1984, hereafter PT84). Quasi-periodic oscillations with various frequencies were also reported (Stella, White, & Priedhorsky 1987b; Hasinger & van der Klis 1989; Smale, Zhang, & White 1997; Zhang et al. 1998; Wijnands, van der Klis, & Rijkhorst 1999; Kaaret et al. 1999).

Whereas the X-ray observations show an 11 minute sinusoidal-like, small amplitude ( $\sim 3\%$  peak to peak) modulation, Anderson et al. (1997) discovered a large  $\sim 16\%$  (peak to peak) modulation (period  $687.6 \pm 2.4$  s) in the UV band (wavelength in the 126–251 nm range) from the *Hubble Space Telescope* (*HST*). The modulation may come from the variable thickness of the outer disk rim (Stella et al. 1987a). The stability of the period [ $\dot{P}/P = (-5.3 \pm 1.1) \times 10^{-8} \text{ yr}^{-1}$ ; van der Klis et al. 1993b] makes it certain that the 685 s modulation is the orbital period. However, the negative period derivative is inconsistent with the lower limit ( $\dot{P}/P > +8.8 \times 10^{-8} \text{ yr}^{-1}$ ) of the standard scenario proposed by Rappaport et al. (1987).

The 4U 1820–30 luminosity variation was first discovered by Canizares & Neighbours (1975), and its possible  $\sim 176$  day periodicity was first reported by PT84. The fact that X-ray bursts have been seen only in the low-luminosity state (Clark et al. 1977; Stella, Kahn, & Grindlay 1984) indicates that the long-term modulation is an intrinsic change in the accretion rate rather than an extrinsic absorp-

tion. However, significant phase shifts from the expected minima predicted by the ephemeris of the  $176.4 \pm 1.3$  day period proposed by PT84 have been observed from *EXOSAT* (Haberl et al. 1987) and *Ginga* (Sansom et al. 1989). The  $\sim 176$  day periodicity, if stable, of the luminosity variation implies (Grindlay 1988) that 4U 1820–30 may be a hierarchical triple in which a third companion star with a period of  $\sim 1.1$  day orbits the 11 minute binary and thereby induces an inner binary eccentricity precession (Mazeh & Shaham 1979) with a period of  $\sim 176$  days.

In this paper, we describe our *Rossi X-Ray Timing Explorer* (*RXTE*) 1996–1997 Proportional Counter Array (PCA) and 1996–2000 All-Sky Monitor (ASM) observations of 4U 1820–30 (§ 2) and report the timing analysis of the data (§ 3), including the 11 minute binary periodicity, phase jitter, period stability, updated quadratic ephemeris, and search for the  $\sim 1.1$  day period that could be associated with a third companion. Analysis of the *RXTE* ASM data gives a new “176 day” modulation ephemeris that connects all the observations from 1969 to 2000 and exhibits no significant period derivative. In § 4, we discuss possible models for the observed light-curve behavior of 4U 1820–30.

### 2. *RXTE* OBSERVATIONS

The *RXTE* PCA/High-Energy X-Ray Timing Experiment (HEXTE) pointed observations of 4U 1820–30 were made on 1996 October 26, 28, and 30 and at least once per month between 1997 February and September. The observation time interval spanned about two 176 day luminosity cycles. Details of the *RXTE* PCA/HEXTE observations are listed in Table 2 in Bloser et al. (2000). The data used for the analysis are in PCA (PCU 0 and 1) Standard-2 format with a time resolution of 16 s. We divide the data into four energy bands, 1.72–3.18, 3.18–5.01, 5.01–6.84, and 6.84–19.84 keV. Since our timing analysis did not suggest any significant energy dependence of the patterns observed, we will present in this paper only the analysis results for band 4 (6.84–19.84 keV) unless otherwise specified. A typical PCA Standard-2 light curve is shown in Figure 1. A complete

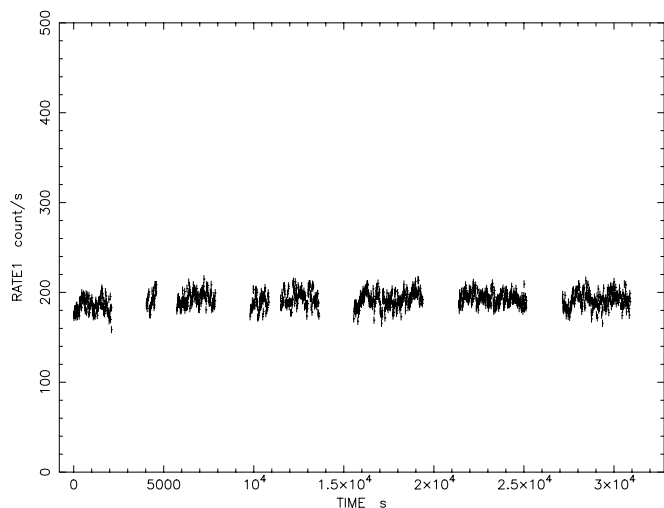


FIG. 1.—Light curve of 4U 1820–30 (6.84–19.84 keV) observed by *RXTE* PCA on 1996 October 28/29.

analysis of the spectra and spectral variations of 4U 1820–30 for these *RXTE* observations is presented by Bloser et al. (2000).

Data for the 4U 1820–30 *RXTE* ASM X-ray light curve (2–12 keV) analyzed in this paper were collected from 1996 January 11 to 2000 March 2 (Fig. 2). The observation window (1576 days) spanned about nine contiguous 176 day modulation cycles. In each modulation cycle, the count rate varies from  $\sim 5$  to  $\sim 35$  counts  $s^{-1}$ .

### 3. DATA ANALYSIS

#### 3.1. Binary Periodicity and Phase Analysis

All *RXTE* PCA data were first corrected for the barycenter arrival times. In order to avoid the possible alias from the  $\sim 176$  day period long-term modulation, we removed the DC term from the observed light curve. We carried out a  $\chi^2$  analysis of the folded light curves (32 bins per period) to search for the best period near 685 s for all

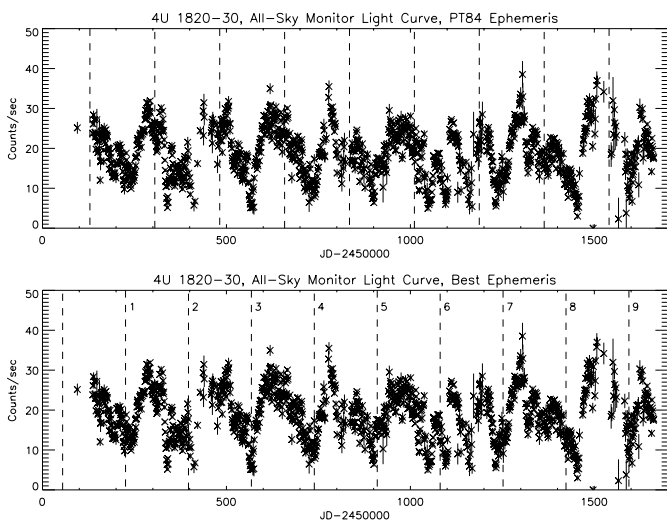


FIG. 2.—4U 1820–30 light curve observed by *RXTE* ASM from 1996 January 11 to 2000 March 2. The dashed lines are the expected minimum intensity times for the ephemeris from PT84 (*top*) and ephemeris of eq. (9) in § 3.3 (*bottom*).

the 4U 1820–30 *RXTE* PCA data. The maximum  $\chi^2$  (deviation of folded light curve from constant flux) is at 685.014 s, as shown in Figure 3. Fitting the 685.014 s peak with a Gaussian returns a best period of  $685.0144 \pm 0.0054$  s. The sidebands are primarily artifacts of the alias period from the observation gaps.

For comparison with historical results, we folded the light curve of each observation by the ephemeris from Tan et al. (1991):

$$T_N^{\max} = \text{HJD } 2,442,803.63544 + \left( \frac{685.0118}{86,400} \right) \times N, \quad (1)$$

where  $N$  is the cycle count. The phase corresponds to the maximum of the sinusoidal fit of each folded light curve. A typical folded light curve is shown as Figure 4. Figure 5 shows the phases of the *RXTE* 1996–1997 observations. The phase of maximum flux are scattered around  $-0.2$  with  $\sim 0.061$  (rms) phase jitter.

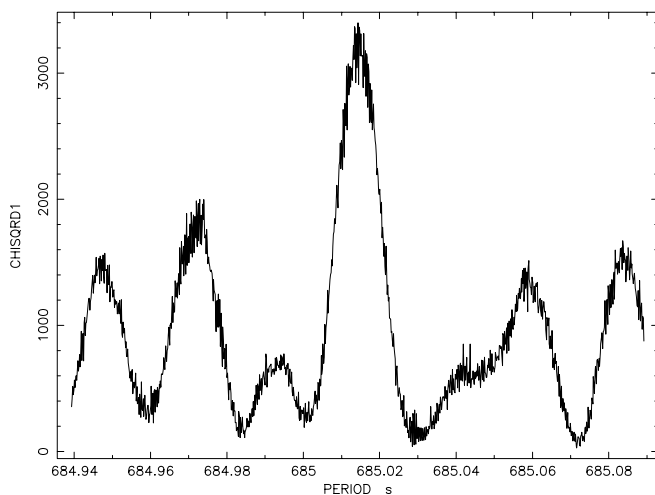


FIG. 3.—Result of  $\chi^2$  folded period searching of the *RXTE* PCA 1996–1997 observation. The Gaussian fit of the peak near 685.01 s yields a best period of  $685.0144 \pm 0.0054$  s.

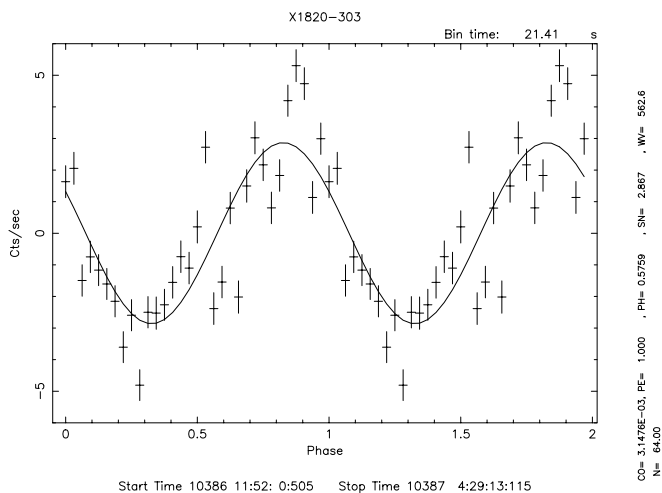


FIG. 4.—Folded light curve of the observation on 1997 September 10 folded by eq. (1) and with the DC flux subtracted. The maximum of sinusoid fit is at about phase 0.8 (or  $-0.2$ ). Interdip is observed at phase 0.5–0.6.

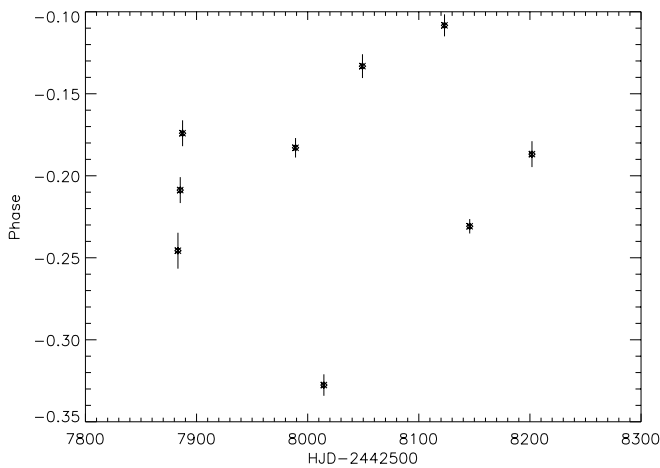


FIG. 5.—Phases of the 4U 1820–30 *RXTE* PCA 1996–1997 observation. The mean fluctuation of the phases is about 0.061.

To update the ephemeris, we appended the mean arrival times from the *RXTE* observations to the historical results from *SAS 3* (Morgan et al. 1988), *Ariel V* (Smale et al. 1987), *Einstein* (Morgan et al. 1988), *Tenma* (Sansom et al. 1989), *EXOSAT*<sup>1</sup> (Stella et al. 1987a), *Ginga* (Sansom et al. 1989; Tan et al. 1991; van der Klis et al. 1993a), and *ROSAT* (van der Klis et al. 1993a, 1993b). The phase (or arrival time offset) errors, however, need to be reestimated. Van der Klis et al. (1993b) discovered the phase shifts about 0.038 in the three *ROSAT* observations in 1991 and 1993 and the historical phase jitter  $\sim 0.050$  around the best-fit linear ephemeris. For the *RXTE* data in this paper, we found that the phase jitter is  $\sim 0.061$  ( $=0.00048$  days). Therefore, an additional 0.061 phase error was quadratically added to the historical data. For the *RXTE* data, we weighted-averaged the phases from each observation for the 1996 and 1997 data sets separately. We calculated the mean phases errors from quadratically adding the 0.061 phase jitter to the average phase errors from a sinusoidal fit of the folded light curves. The resulting mean phases are  $-0.20259 \pm 0.0613$  and  $-0.20352 \pm 0.0612$  for the 1996 and 1997 data sets, respectively. The mean arrival time for the average phases of two data sets were obtained from the expected flux maxima of the midobservation times of the observation windows; that is,

$$T_{\text{mean}} = T_0 + P_{\text{fold}} \times (N_{\text{mid}} + \phi_{\text{ave}}), \quad (2)$$

where  $T_0 = \text{HJD } 2,442,803.63544$ ,  $P_{\text{fold}} = (685.01180/86,400)$  days,  $N_{\text{mid}}$  is the cycle number closest to the midtime of the data set, and  $\phi_{\text{ave}}$  is the mean phase for the 1996 and 1997 observations.

The period derivative can be obtained from a quadratic fit:

$$\Phi = \Phi_0 + \frac{\Delta P}{(P_{\text{fold}})^2} t + \frac{1}{2} \frac{\dot{P}}{(P_{\text{fold}})^2} t^2. \quad (3)$$

We applied linear ( $\dot{P} = 0$ ) and quadratic fits to the data. Both fits give acceptable results:  $\chi^2 = 12.47$  (dof = 21) for

<sup>1</sup> Arrival time errors of 0.0002 days were quadratically added; see van der Klis et al. (1993a).

the linear fit and  $\chi^2 = 6.96$  (dof = 20) for the quadratic fit. However, the *F*-test (Bevington 1992) shows that  $F(\nu_1 = \Delta\nu = 1; \nu_2 = 20) = 15.83$  for linear and quadratic fits. This implies that the quadratic fit is better than the linear fit at the  $\sim 99.99\%$  confidence level. Thus, the quadratic ephemeris is still required.

From the quadratic fit of the data (Fig. 6), we obtained  $\dot{P} = (-7.54 \pm 3.21) \times 10^{-13} \text{ s s}^{-1}$  or  $\dot{P}/P = (-3.47 \pm 1.48) \times 10^{-8} \text{ yr}^{-1}$ , which is consistent with the value found by van der Klis et al. (1993b). The quadratic ephemeris<sup>2</sup> can be written as

$$T_N = \text{HJD } 2,442,803.63564 \pm 2.2 \times 10^{-4} \\ + \left( \frac{685.0119 \pm 1.02 \times 10^{-4}}{86,400} \right) \times N \\ + (-2.99 \pm 1.27) \times 10^{-15} \times N^2. \quad (4)$$

Tan et al. (1991) showed that the 685 s modulation phases are well fitted by a period of  $\sim 8.5 \pm 0.2$  yr sinusoidal curve from the 1976–1989 observation results. The period may be real or an artifact from the observation gap between 1981 and 1984 (Tan et al. 1991). To clarify the ambiguity, we used the constant-sinusoidal, linear-sinusoidal, and quadratic-sinusoidal models to fit the phases from all the 1976–1997 observations near the 8.5 yr period. The  $\chi^2$  minimum fit results for the three different models are listed in Table 1. Although the linear-sinusoidal and the quadratic-sinusoidal models gave smaller reduced  $\chi^2$  values than the quadratic model, the fitted amplitudes for both cases were only  $\sim 0.05$  (modulation period  $\sim 6.5$  yr), less than the 0.06 phase jitter. Therefore, there is no significant long-term phase periodic

<sup>2</sup> The small offset due to leap seconds was ignored in our data analysis. The offset is about 16 s from phase 0 epoch (JD 2,442,803) to the end of the observations (1997 September 9 = JD 2,450,701). If we assume that the offset drifts linearly with time (first-order approximation), this systematic effect will give only a  $1.6 \times 10^{-5}$  s offset in the second term of eq. (4). It is much smaller than the error ( $1.02 \times 10^{-4}$  s) from the quadratic fit. The periodic systematic effect due to the difference between the heliocentric time and the barycentric time ( $\sim 2.5$  s, mainly determined by the position of Jupiter) was also neglected.

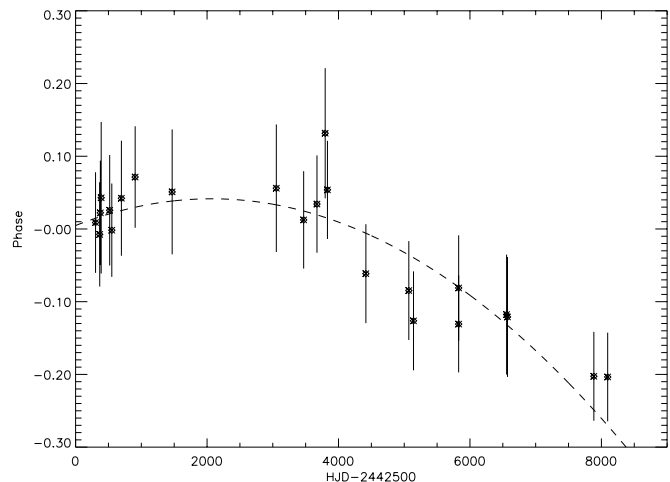


FIG. 6.—Phases of the 4U 1820–30 11 minute modulation from the 1976–1997 observation folded by the ephemeris of eq. (1). The dashed line represents the best quadratic fit result.

TABLE 1  
PHASE MODULATION FIT RESULTS

Model	Reduced $\chi^2$	Period from Sinusoidal Fit (day)	Amplitude from Sinusoidal Fit
Linear .....	0.594	...	...
Quadratic .....	0.349	...	...
Constant + sinusoidal near $P = 8.5$ yr .....	0.782	$2978.3 \pm 140.7$	0.0965
Linear + sinusoidal near $P = 8.5$ yr .....	0.315	$2475.9 \pm 224.8$	0.0567
Quadratic + sinusoidal near $P = 8.5$ yr .....	0.223	$2368.9 \pm 267.0$	0.0446

modulation of period  $\sim 6$ –8 yr, and the  $\sim 6.5$  yr “period” is highly likely to be an artifact from the phase jitter and the observation gaps between 1976 *SAS 3* and 1985 *EXOSAT* ( $\sim 3500$  days, 1.5 period), 1985 *EXOSAT* and 1989 *Ginga* ( $\sim 1300$  days, 0.5 period), and 1989 *Ginga* and 1991 *ROSAT* ( $\sim 1400$  days, 0.5 period) observations.

In explaining the discrepancy between the positive period derivative predicted by the standard scenario versus the negative observed  $\dot{P}$ , van der Klis et al. (1993b) demonstrated that the negative phase shift could be due to a long-term variation of the disk size. The proposal can be tested by looking for a dependence of orbital phase on  $\dot{M}$  (van der Klis et al. 1993b), or  $L_X$ . We compared the 11 minute modulation phases from the 1996–1997 the *RXTE* observations and the simultaneous count rates from the *RXTE* ASM (except the 1997 February 9 observation, which has no ASM data). The linear correlation coefficient is only 0.17, which implies that the uncorrelated probability is about 70%. Therefore, no significant correlation between binary orbital phases and luminosities is observed. Further considerations about the phase shift are given in § 4.

### 3.2. Possible Period Sidebands

Grindlay (1986, 1988) suggested that the period of  $\sim 176$  day long-term modulation of 4U 1820–30 (PT84) may be due to a hierarchical triple companion star (captured by the compact binary in the high-density cluster core) which modulates the eccentricity of the inner binary at a long-term period  $P_{\text{long}} = KP_{\text{outer}}^2/P_{\text{inner}}$ , where  $P_{\text{inner}}$  and  $P_{\text{outer}}$  refer to the binary period and the orbital period of the third companion and  $K$  is a constant of order unity which depends on mass ratios and relative inclinations (Mazeh & Shaham 1979). Under the triple model, with 176 day long-term modulation and 685 s binary orbital period, the theoretical orbital period of the third star in the 4U 1820–30 system would be  $\sim 1.1$  days (for  $K \simeq 1$ , however, factors of 2 smaller or larger periods for the triple companion could be accommodated for differing inclination). If 4U 1820–30 is a triple system, the 685 s modulations would be affected by such a period and the beat sidebands should appear near the peak of the power spectrum. We considered the binary motion around the center of mass of triple system. For the third companion star of mass  $\sim 0.5 M_{\odot}$  (approximate maximum allowed by the optical counterpart) and  $\sim 1.1$  day orbital period, the radius of the binary motion relative to the center of mass of triple system is only  $\sim 3.4 \sin i_3$  lt-s, where  $i_3$  is the inclination angle of the orbit of triple companion. In other words, the observed  $\sim 1.1$  day period phase modulation amplitude is no more than  $5 \times 10^{-3}$ . Although the phase variation from the binary motion may be too small to be observed, the third companion star could still affect the light curve in other ways. If, for example, the

third companion star makes the 11 minute modulation amplitude change,  $\sim 1.1$  day beat sidebands<sup>3</sup> amplitudes may be detectable in the Fourier spectrum.

To search possible sidebands, we considered only the 1996 October 26–30 light curves because the observation gaps for the 1997 observations were too significant. To further minimize the observation windows (from observation gaps and Earth occultation), a one-dimensional CLEAN algorithm described by Roberts, Lehar, & Dreher (1987) was applied to convert for the unequally spaced observations. We searched an arbitrary wide frequency range between  $1.38 \times 10^{-3}$  Hz ( $P = 724.6$  s) and  $1.55 \times 10^{-3}$  Hz ( $P = 645.2$  s) with amplitudes at greater than  $2 \sigma$  significance. The search results are shown as Figure 7. Only one primary peak is observed. The peak has an amplitude of  $2.42 \pm 0.26$  counts  $\text{s}^{-1}$  and a period of 685.120 s. There are no other significant sidebands beside this primary peak.

<sup>3</sup> The beat sideband periods  $P_{\text{beat}} = (1/P_{\text{inner}} \pm n/P_{\text{outer}})^{-1}$ , where  $n$  is a positive integer and  $P_{\text{inner}}$  and  $P_{\text{outer}}$  are the binary (11 minutes) and third star periods ( $\sim 1.1$  days), respectively. The first harmonic ( $n = 1$ ) beat sideband periods are thus 689.97 s ( $f = 1.45 \times 10^{-3}$  Hz) and 680.10 s ( $f = 1.47 \times 10^{-3}$  Hz). The apparent sideband peak in the top plot of Fig. 7 are tantalizing but is probably due to the  $\sim 1$  day spacing between successive observations. A longer continuous observation would be required to remove these alias peaks.

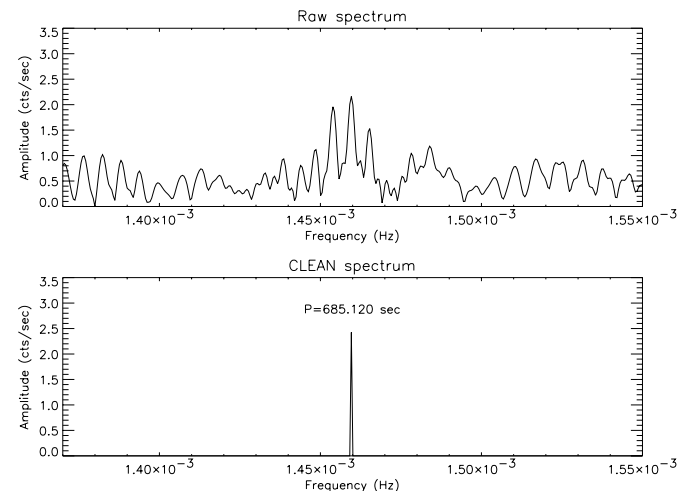


FIG. 7.—Raw (top) and CLEANed (bottom) Fourier amplitude (i.e., absolute values of the Fourier transformation) spectra of *RXTE* 1996 October observations. The upper amplitude limit for the CLEAN spectrum is 0.52 counts  $\text{s}^{-1}$  ( $2 \sigma$ ). There is no clear sideband beside the peak; therefore, the sidebands in the raw spectrum are likely artifacts from  $\sim 1$  day observation gaps.

### 3.3. $\sim 176$ Days Modulation

The 1 day average binned light curve for the *RXTE* ASM data (see Fig. 2) shows a clear modulation with relatively rapid rise and slow fall in count rate with a  $\sim 176$  day period. The count rate varies from 5 to 35 counts  $s^{-1}$  (see Fig. 2) throughout each cycle. “Interdips” were also observed between the first and second, fourth and fifth, fifth and sixth, and sixth and seventh minima of the *RXTE* ASM light curve (minimum cycle count indices are marked on the bottom plot of Fig. 2).

PT84 reported the 4U 1820–30 long-term modulation period to be  $176.4 \pm 1.3$  days. However, the ephemeris from PT84 [ $T_{\min} = \text{JD } 2,442,014.5 + (176.4 \pm 1.3) \times N$ ] does not match the *EXOSAT* 1985 August 19/20 4U 1820–30 low-state observation (Haberl et al. 1987), where the expected minimum (by ephemeris from PT84) was offset by 48 days. A similar discrepancy was found in the data from the *Ginga* ASM (delayed by  $\sim 50$  days; Sansom et al. 1989; S. Kitamoto 2000, private communication). The light curve of the *RXTE* ASM data also shows a  $\sim 0.45$  (80 day) phase shift (see top plot of Fig. 2). The inconsistency may be caused by an incorrect ephemeris (phase 0 epoch, period, or both) or a period drift.

To obtain the best period to describe the 4U 1820–30 *RXTE* ASM light curve, we first applied a fast Fourier transformation (FFT). However, because the observation window is only a brief  $\sim 8.8$  cycles (1576 days), the FFT frequency resolution,  $\delta f = 1/(1576 \text{ days}) = 0.233 \text{ cycles yr}^{-1}$ , yields the period resolution near 176 days of  $\delta P \approx P^2 \times \delta f = 19.8 \text{ days}$ , which is too coarse for  $\sim 176$  day period modulation. Therefore, the interpolated Fourier transformation (Middleditch, Deich, & Kulkarni 1993) was applied to further determine the best period. The FFT is only able to show amplitudes of the “integer” frequencies ( $f_n = n/T$ , where  $n$  is an integer and  $T$  is the total time of the data) whereas the interpolated Fourier may show the amplitude of “noninteger” frequencies ( $f_r = r/T$ , where  $r$  is any real number). The noninteger amplitude  $A_r$  can be estimated from the locally neighboring Fourier amplitudes as

$$A_r \sim \sum_{l=[r]-m}^{[r]+m} A_l e^{-i\pi(r-l)} \frac{\sin(\pi(r-l))}{\pi(r-l)}, \quad (5)$$

where  $m$  is integer and  $[r]$  denotes the nearest integer of  $r$ . The uncertainty of peak frequency

$$\sigma_f = \frac{3}{\pi \alpha T \sqrt{6P_0}}, \quad (6)$$

where

$$\alpha = \frac{1}{\pi T} \sqrt{-\frac{3}{2P_0} \frac{\partial^2 P}{\partial f^2}}, \quad (7)$$

$P_0$  is the peak power, and  $T$  is the length of the observation window (Middleditch et al. 1993).

We chose  $m = 2$  and the resolution of  $r$  to be 0.1. The interpolated Fourier transformation spectrum is shown in the bottom plot of Figure 8. The peak amplitude was observed at  $f = 2.130 \text{ cycles yr}^{-1}$  with a value of 4.506 counts  $s^{-1}$ . The frequency uncertainty from equation (6) and equation (7) is  $0.0240 \text{ cycles yr}^{-1}$ , where the second derivative in equation (7) is estimated by the quadratic fit around the peak of the power spectrum. Therefore, the best

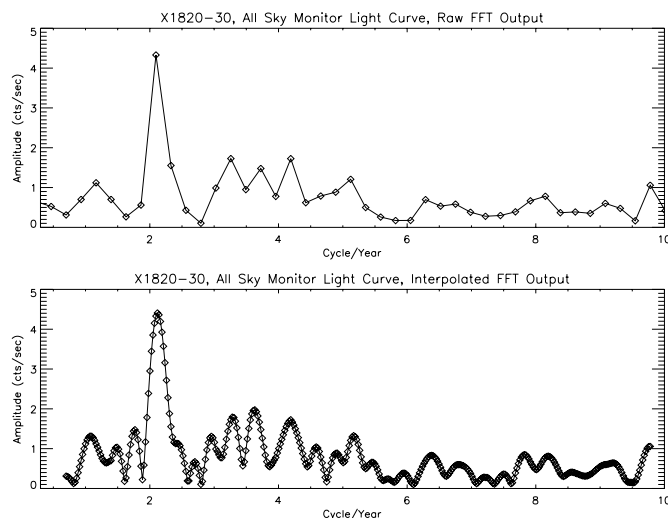


FIG. 8.—Raw FFT spectrum (top) and interpolated Fourier spectrum (bottom) of the 4U 1820 *RXTE* ASM light curves.

4U 1820–30 long-term modulation period for the *RXTE* ASM data is  $171.39 \pm 1.93$  days. Furthermore, the  $\chi^2$  period searching method gave the best period of 171.23 days ( $\pm 7.36$  days), close to the interpolated Fourier transformation result.

The *RXTE* ASM light curve, derived by folding at a period of 171.39 days (see Fig. 9), shows that the minimum closest to the middle of observation is at JD 2,450,907.96 and  $\pm 0.07$  (rms) phase jitter (or  $\pm 12$  days). The best linear ephemeris to describe the intensity minimum of the *RXTE* ASM light curve (hereafter “local ephemeris”) can be written as

$$T_{\min}^{RXTE} = \text{JD } 2,450,907.96 \pm 12.00 \\ + (171.39 \pm 1.93) \times N. \quad (8)$$

To obtain the best linear ephemeris for the intensity minimum in the *RXTE* ASM light-curve and historical data, we assigned an uncertainty of  $\pm 12$  days (from the 0.07 phase jitter obtained from the *RXTE* ASM light curve) to the minimum time reported by PT84 (JD 2,442,014.5).

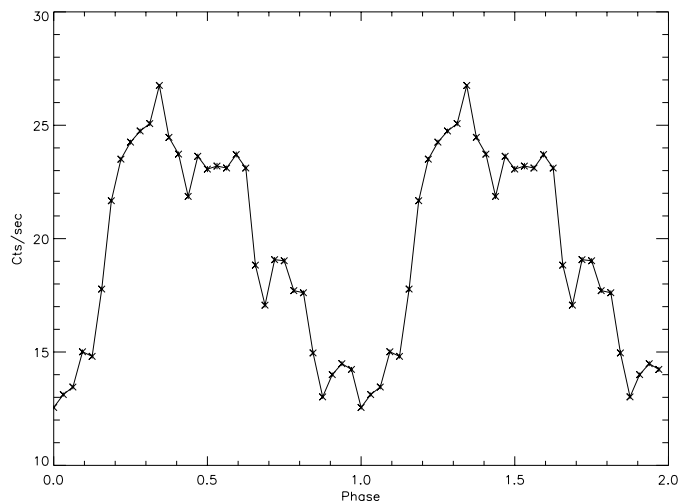


FIG. 9.—4U 1820–30 *RXTE* ASM light curve folded by the local ephemeris (eq. [8]).

TABLE 2  
X-RAY BURST PHASES

Observation Date	Julian Date	Phase Folded by PT84 Ephemeris	Phase Folded by Equation (9)	Reference
1975 May 18 .....	2,442,550.5	0.039	0.124	1
1975 Sep 28 .....	2,442,683.5	−0.207	−0.098	2
1976 Mar 15 <sup>a</sup> .....	2,442,852.5	−0.250	−0.110	3
1985 Aug 20 .....	2,446,297.5	0.280	0.032	4

<sup>a</sup> Midobservation date of 1976 March 11.5–19.5.

REFERENCES.—(1) Clark et al. 1976; (2) Grindlay et al. 1976; (3) Clark et al. 1977; (4) Haberl et al. 1987.

Combined with intensity minimum times observed by the *Ginga* ASM (JD 2,446,822 ± 26; S. Kitamoto 2000, private communication) and *RXTE* ASM data, the linear fit yields the best historical ephemeris of

$$T_{\min} = \text{JD } 2,450,909.90 \pm 11.66 \\ + (171.033 \pm 0.326) \times N. \quad (9)$$

The expected intensity minimum times from equation (9) versus the *RXTE* ASM light curve are shown as the bottom plot of Figure 2. An independent check on the ephemeris may be derived from timing of X-ray burst activity. Stella et al. (1984, and references therein) reported that no bursts are detected in the high state, which implies that the “burst phase” should be near phase 0. Table 2 lists the observation dates with bursts being detected and the phases of these days. No burst phase folded by equation (9) exceeded the range of ±0.13 (±23 days). This indicates that the long-term modulation period of 4U 1820–30 is close to 171.033 days and stable over ~30 yr.

To estimate the period derivative (or its upper limit), we suppose the minimum times ( $T_N$ ) obey a quadratic ephemeris (for small  $\dot{P}$ )

$$T_N = T_0 + P_0 N + \frac{1}{2} P_0 \dot{P} N^2, \quad (10)$$

where  $N$  is cycle count index. Taking the phase 0 epoch  $T_0$  to be that in equation (8) (JD 2,450,907.96), since the cycle numbers are small for *RXTE* intensity minima (from −4 to 4), the quadratic term in equation (10) can be neglected. Equation (10) is reduced to a linear ephemeris equal to the local ephemeris (i.e., eq. [8]). The phases of historical data (*Vela 5B* and *Ginga*) folded by equation (8) should be due to the period derivative

$$\Phi = \frac{1}{2} \frac{\dot{P}}{(P_0)^2} \Delta t^2, \quad (11)$$

where  $\Delta t$  is time difference between minimum time and  $T_0$ . Applying equation (8) to historical data, we found no significant period derivative. The 2  $\sigma$  (90%) confidence level upper limit for the change in the 171 day period is  $|\dot{P}| < 1.03 \times 10^{-4} \text{ days day}^{-1}$  (=0.038 days yr<sup>−1</sup>) or  $|\dot{P}/P| < 2.20 \times 10^{-4} \text{ yr}^{-1}$ . This stable long-term modulation is consistent with 4U 1820–30 being a hierarchical triple system with a ~1.1 day period companion.

#### 4. DISCUSSION

The observed negative period derivative from the 4U 1820–30 *RXTE* 1996–1997 observations combined with all the historical data is consistent with the previous conclusions proposed by Tan et al. (1991) and van der Klis et al. (1993a, 1993b). The decreasing 685 s period deviates from the positive  $\dot{P}$  ( $\dot{P}/P > 8.8 \times 10^{-8} \text{ yr}^{-1}$ ) predicted by the standard scenario (Rappaport et al. 1987). Tan et al. (1991)

suggested that the discrepancy is probably caused by the acceleration of the binary star by the gravitational potential of the globular cluster. On the other hand, by analyzing the theoretical minimum of the period derivative, van der Klis et al. (1993a) found that the gravitational acceleration by the globular cluster is not enough to explain the observed results even if the line of sight is very close to the line connecting the binary with the center of the cluster at the projected separation of 4'' ± 1''.

However, King et al. (1993) measured the NGC 6624 cluster center with the *HST* Faint Object Camera and discovered that 4U 1820–30 is 0".66 from the cluster center. For an assumed distance of 6.4 kpc (Vacca, Lewin, & van Paradijs 1986; Haberl & Titarchuk 1995), this is equivalent to only 0.02 pc (projected) from the core. Using the model proposed by van der Klis et al. (1993a), we find that the maximum gravitational acceleration along the line of sight could be  $a/c = 2.5 \times 10^{-15} \text{ s}^{-1}$ . Combining the period derivative derived in § 3.1 and its value from the standard scenario, we determined the acceleration along the line of sight to be  $a/c = 3.9 \times 10^{-15} \text{ s}^{-1}$ , only ~50% larger than the maximum value. Therefore, given the uncertainties in both  $\dot{P}$  and the cluster acceleration (i.e., center and mass model), gravitational acceleration by the globular cluster is still a possible explanation for the negative period derivative (also see King et al. 1993).

Another potential explanation of the negative period derivative (or negative phase shift) was proposed by van der Klis et al. (1993b). The 685 s intensity modulation of the 4U 1820–30, as for the dipping sources, is probably caused by the occultation by the accretion stream of the vertical structure at the edge of the accretion disk (Stella et al. 1987a; Morgan et al. 1988; Sansoni et al. 1989; van der Klis et al. 1993b). The azimuth point of impact depends on the disk size. The bulge on the disk rim could shift by as much as ~−120°, larger than the observed phase shifts of ~−72° (−0.2 phase, the approximate value needed to account for the negative  $\dot{P}$ ). However, if we consider only the standard scenario,  $\dot{P}/P \sim 8.8 \times 10^{-8} \text{ yr}^{-1}$ , the phase shift resulting from the period change is expected to be ~+0.75 from the 1976 *SAS* 3 to the 1997 *RXTE* observations. This result implies that the total bulge phase shift is ~−0.95 (−350°). The bulge is unlikely to have such a large phase shift. Furthermore, the disk size should be highly correlated with the accretion rate and, of course, the luminosity  $L_X$ . As discussed in § 3.1, no significant correlation between orbital phase and luminosity (171 day variation) is found in the *RXTE* 1996–1997 data. We hence conclude that the negative phase shift is unlikely to be caused by a variation of the disk size.

In this paper, we derived the long-term modulation period and showed from the ephemeris (eq. [9]) that the 4U 1820–30 bursts are observed only in the low state.

By reanalyzing the historical data as well as tabulated burst activity time, we derived a period  $P = 171.033 \pm 0.326$  days and a limit on  $|\dot{P}| < 1.03 \times 10^{-4}$  days day $^{-1}$ . The high correlation between the burst activity and the luminosity suggests that the 171 day modulation is stable and indeed an intrinsic luminosity change rather than an extrinsic periodic obscuration. This luminosity modulation and (primarily) its long-term stability supports earlier suggestions for a hierarchical triple companion. The mass transfer rate is very sensitive to the Roche lobe radius, which is proportional to the inner binary separation. A hierarchical companion third star will induce an eccentricity variation in the inner (11 minutes) binary with a period  $P_{\text{long}} = KP_{\text{outer}}^2/P_{\text{inner}}$  (Mazeh & Shaham 1979). When the minimum separation of the inner binary is small, the mass transfer rate and luminosity changes are enhanced. The triple model to 4U 1820–30 system implies that a  $\sim 1.1$  day period third companion is responsible for the 171.033

day long-term intensity modulation. The triple companion star affects the orbital motion of the inner binary through beats of the 685 s binary period and the  $\sim 1.1$  day companion star orbital period. Our *RXTE* observations were not sensitive to this because of both data sampling ( $\sim 1$  day observation gaps) and the small amplitude expected. An additional test of the triple model could be conducted by a continuous, or optimally sampled, long ( $\gtrsim 3$ –10 days) observation of 4U 1820–30 to measure the small ( $\sim 3.4 \sin i_3$  lt-s; see § 3.2) phase shifts, or the possible modulation sidebands (Fig. 7) without 1 day sampling alias effects.

The authors thank S. Kitamoto for invaluable assistant with the *Ginga* data, *RXTE*-GOF for help with *RXTE* data analysis, and the HEASARC for archival *RXTE* data. This work was supported in part by NASA grant NAG5-3293 and NAG5-7393.

## REFERENCES

- Anderson, S. F., et al. 1997, *ApJ*, 482, L69  
 Bevington, P. R. 1992, *Data Reduction and Error Analysis for the Physical Sciences* (New York: McGraw-Hill)  
 Bloser, P. F., Grindlay, J. E., Kaaret, P., Zhang, W., Smale, A. P., & Barret, D. 2000, *ApJ*, 542, 1000  
 Canizares, C. R., & Neighbours, J. E. 1975, *ApJ*, 199, L97  
 Clark, G. W., et al. 1976, *ApJ*, 207, L105  
 ———, 1977, *MNRAS*, 179, 651  
 Grindlay J. E. 1986, in *The Evolution of Galactic X-Ray Binaries*, ed. J. Trumper, W. Lewin, & W. Brinkman (NATO/ASI Ser. C, 167; Dordrecht: Kluwer), 25  
 ———, 1988, in *IAU Symp. 126, Globular Cluster System in Galaxies*, ed. J. E. Grindlay & A. G. Davis Philip (Dordrecht: Reidel), 347  
 Grindlay J. E., et al. 1976, *ApJ*, 205, L127  
 ———, 1984, *ApJ*, 282, L13  
 Haberl, F., et al. 1987, *ApJ*, 314, 266  
 Haberl, F., & Titarchuk, L. 1995, *A&A*, 299, 414  
 Hasinger, G., & van der Klis, M. 1989, *A&A*, 225, 79  
 Kaaret, P., et al. 1999, *ApJ*, 520, L37  
 King, I. R., et al. 1993, *ApJ*, 413, L117  
 Mazeh, T., & Shaham, J. 1979, *A&A*, 77, 145  
 Middleditch, J., Deich, W., & Kulkarni, S. 1993, in *Isolated Pulsars*, ed. K. A. Van Riper, R. I. Epstein, & C. Ho (Cambridge: Cambridge Univ. Press), 372  
 Morgan, E. H. Remillard, R. A., & Garcia, M. R. 1988, *ApJ*, 324, 851  
 Priedhorsky, W., & Terrell, J. 1984, *ApJ*, 284, L17 (PT84)  
 Rappaport, S., et al. 1987, *ApJ*, 322, 842  
 Roberts, D. H., Lehar, J., & Dreher, W. 1987, *AJ*, 93, 968  
 Sansom, A. E., et al. 1989, *PASJ*, 41, 591  
 Smale, A. P., Mason, K. O., & Mukai, K. 1987, *MNRAS*, 225, 7P  
 Smale, A. P., Zhang, W., & White, N. E. 1997, *ApJ*, 483, L119  
 Stella, L. Kahn, S. M., & Grindlay J. E. 1984, *ApJ*, 282, 713  
 Stella, L., Priedhorsky, W., & White, N. E. 1987a, *ApJ*, 312, L17  
 Stella, L., White, N. E., & Priedhorsky, W. 1987b, *ApJ*, 315, L49  
 Tan, J., et al. 1991, *ApJ*, 374, 291  
 Vacca, W. D., Lewin, W. H. G., & van Paradijs, J. 1986, *MNRAS*, 220, 339  
 van der Klis, M., et al. 1993a, *MNRAS*, 260, 686  
 ———, 1993b, *A&A*, 279, L21  
 Wijnands, R., van der Klis, M., & Rijkhorst, E. 1999, *ApJ*, 512, L39  
 Zhang, W., et al. 1998, *ApJ*, 500, L171